Journal of Sound and Vibration 328 (2009) 396–410

Contents lists available at ScienceDirect

Journal of Sound and Vibration

journal homepage: www.elsevier.com/locate/jsvi

Prediction and validation of the energy dissipation of a friction damper

I. Lopez *, H. Nijmeijer

Section Dynamics and Control, Department of Mechanical Engineering, Eindhoven University of Technology, P.O. Box 513, 5600 MB Eindhoven, The Netherlands

ARTICLE INFO

Article history:
Received 22 March 2009
Received in revised form
18 August 2009
Accepted 19 August 2009
Handling Editor: M.P. Cartmell
Available online 12 September 2009

ABSTRACT

Friction dampers can be a cheap and efficient way to reduce the vibration levels of a wide range of mechanical systems. In the present work it is shown that the maximum energy dissipation and corresponding optimum friction force of friction dampers with stiff localized contacts and large relative displacements within the contact, can be determined with sufficient accuracy using a dry (Coulomb) friction model. Both the numerical calculations with more complex friction models and the experimental results in a laboratory test set-up show that these two quantities are relatively robust properties of a system with friction. The numerical calculations are performed with several friction models currently used in the literature. For the stick phase smooth approximations like viscous damping or the arctan function are considered but also the non-smooth switch friction model is used. For the slip phase several models of the Stribeck effect are used. The test set-up for the laboratory experiments consists of a mass sliding on parallel ball-bearings, where additional friction is created by a sledge attached to the mass, which is pre-stressed against a friction plate. The measured energy dissipation is in good agreement with the theoretical results for Coulomb friction.

1. Introduction

Frictional forces arising from the relative motion of two contacting surfaces are a well-known source of energy dissipation. Sometimes this is an unwanted effect of the design, but it can also be intentionally used to increase the damping of a certain system in a simple and cost-effective way.

Friction dampers are used in very diverse applications: civil engineering, rotor machinery (mainly turbines), vehicles and ring dampers. The common goal in these applications is to find the optimum system parameters that lead to the highest amount of damping possible for a given friction damper design. This implies that a model of the system with friction is needed, where the main issue is finding the right friction model for that system. In general the friction models normally applied to friction damping can be divided into micro-slip models, where the contact interface is modeled with a number of friction elements in parallel (see for example [1,2]) and macro-slip models where local contact is assumed and a single friction element is used. This paper focuses on systems with stiff localized contacts and where the relative displacements within the contact are relatively large. These systems do not require an accurate description of the pre-sliding behavior, and can be modeled using a single friction element. The most widespread model in the literature on friction damping is the classical Coulomb friction model (with equal static and dynamic friction forces). In [3] a procedure to design friction dampers for turbine blades is presented based on minimizing the blade stress, while an expression for the

* Corresponding author. Tel.: +31 40 247 2611; fax: +31 40 246 1418.
E-mail address: i.lopez@tue.nl (I. Lopez).

0022-460X/$ - see front matter © 2009 Elsevier Ltd. All rights reserved.
doi:10.1016/j.jsv.2009.08.022

equivalent viscous damping coefficient for a single degree of freedom (SDOF) system with friction is found in [4] using the harmonic balance method. More recently, a study on friction damping applied to an isolation system for buildings has been presented in [5], where the optimum friction force is found by minimizing the response amplitude. In [6] approximate expressions for the energy dissipated per cycle and optimum friction force for a single degree of freedom (SDOF) system with friction are obtained applying the harmonic balance method. The classical Coulomb friction model has also been applied in models for structures connected by a friction damper [7], thin-walled friction dampers for turbine blades [8], damping of conical whirl in rotors [9], friction dampers for vehicle applications [10,11] and friction dampers for railway wheels [12,13].

There are very few works where more complex friction models are used to model friction damping [14–17]. In his review on nonlinear passive vibration isolators [14], Ibrahim discusses friction-pendulum systems, where teflon sliding bearings are used and mentions that the friction coefficient strongly depends on the sliding velocity (Stribeck effect). A model for the Stribeck effect in teflon bearings was presented in [15] and compared to a Coulomb friction model. It was concluded that the use of Coulomb's constant friction model may result in a useful estimation of the peak response, provided that an appropriate value of the coefficient of friction is used. In [16] the friction force is modeled using a Coulomb friction model with different static and dynamic friction forces ($F_s \neq F_d$). It is shown that for $F_s > F_d \geq 0.64F_s$ (which is the range often found in practice [18–22]) the maximum energy dissipation and the corresponding optimum friction force are constant and equal to those obtained with the classical Coulomb friction model. This gives an indication that the choice of friction model might have a limited influence on the predicted maximum energy dissipation. A Stribeck model and numerical simulations have been used in [17] to determine the overall energy levels of two SDOF systems connected by a joint, but the results are not compared to the Coulomb model.

In the light of the literature study the following question arises: How close to reality should the friction model be in order to obtain good estimations of the energy dissipation and optimum system parameters? Or, in other words, is a simple model like the Coulomb model good enough to be applied to the design of friction dampers with stiff localized contacts and large relative displacements?

The goal of the present paper is to investigate whether an accurate friction model is needed to estimate the optimum friction force and maximum energy dissipation correctly and, therefore, to optimize the design of friction dampers. In order to answer these questions a SDOF model of a mass driven by a periodic force has been studied both numerically and experimentally. Several different friction models have been considered in the numerical study. The stick-phase is modeled using continuous approximations (viscous damping, arctan function) and implementations of the Stribeck effect and viscous damping are considered for the slip-phase. The stable periodic solutions have been found using a single-point shooting method. Once the periodic solution is known, the energy dissipated per cycle has been determined. It is shown that the use of continuous approximations to model the stick-phase (viscous damping, arctan function) has limited influence on the predicted energy dissipation and that the exact behavior during the stick-phase will not significantly influence the prediction of the maximum energy dissipation and the optimal friction force. Furthermore the optimum friction force and maximum energy dissipation are relatively insensitive to the choice of friction model in the sliding region, as long as realistic values of the parameters are used. The test set-up for the laboratory experiments consists of a mass sliding on parallel ball-bearings, where additional friction is created by a sledge attached to the mass, which is pre-stressed against a friction plate. No care has been taken to ensure pure dry (Coulomb) friction. Nevertheless, the measured energy dissipation is in good agreement with the theoretical results for Coulomb friction presented in [16], which supports the conclusions from the numerical analysis.

The paper is organized as follows. First the most important definitions and results from [16] are summarized in Section 2. In Section 3 the influence of the friction model is analyzed and the results are discussed. The experimental set-up and data processing are described in Section 4 and in Section 5 the experimental results are presented and compared to the theoretical results. Finally the conclusions are summarized in Section 6.

2. Background

In Fig. 1(a) a SDOF system with friction is shown excited by a periodic harmonic force $f_0(t) = F_0\sin(\omega_0 t)$, where F_0 is the force amplitude and ω_0 the radian frequency. Such a SDOF system is often used to model friction dampers. Here the limiting case $\omega_n/\omega_0 \to 0$ is considered, where $\omega_n = \sqrt{k/m}$ is the natural frequency of the SDOF system. In this case

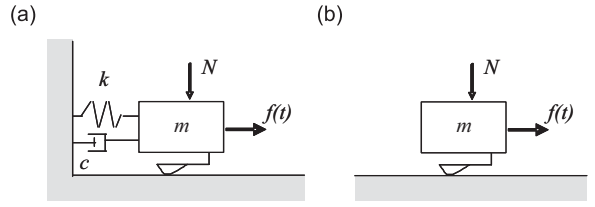

Fig. 1. SDOF system driven by a periodic force. (a) Mass–spring–damper, (b) mass.

the SDOF system reduces to a free mass with friction excited by a periodic force as shown in Fig. 1(b). The free mass system with friction is chosen for its simplicity and ease of implementation (both numerical and experimental). But it can be shown [16] that for $\omega_n/\omega_0<1$ and $\xi_n<0.5$ (ξ_n modal damping ratio) the SDOF system in Fig. 1(a) displays the same qualitative behavior regarding the energy dissipated as function of the friction force as the free mass in Fig. 1(b).

If the classical Coulomb friction model as defined in (1) is used, closed-form expressions for the motion of mass m can be derived and consequently, the energy dissipated per cycle can be determined:

$$F_r = \begin{cases} F_d \operatorname{sgn}(v), & |v|>0, \\ [-F_d, F_d], & |v|=0, \end{cases} \tag{1}$$

where F_r is the friction force and v the velocity of the mass.

The normalized friction force is defined as

$$f_r = \frac{F_r}{F_0}. \tag{2}$$

The motion of the mass in Fig. 1(b) can take several forms depending on the value of the normalized friction force:

$$f_r>1 \quad \text{stick}, \tag{3}$$

$$1>f_r\geq f_r|_{\text{threshold}} \quad \text{stick}-\text{slip}, \tag{4}$$

$$f_r|_{\text{threshold}}>f_r\geq 0 \quad \text{continuous sliding}. \tag{5}$$

The threshold value of the normalized friction force for the transition from stick–slip to continuous sliding is [16]

$$f_r|_{\text{threshold}} = \sqrt{\frac{1}{1+\frac{\pi^2}{4}}} \simeq 0.54. \tag{6}$$

This equation implies that, for a given friction force, the level of excitation force needed to bring the system in continuous sliding is independent of the mass and the excitation frequency. The dissipated energy per period, E_d, can be calculated according to the following expression:

$$E_d = \int_0^T -F_r v(t)\,\mathrm{d}t, \tag{7}$$

where E_d is the energy dissipated per cycle and T the period time of the periodic solution. An expression for the energy dissipation as a function of the friction force has been found in [16] and is plotted in Fig. 2. It is also shown that the normalized optimum friction force and maximum energy dissipation are

$$f_r|_{\max} = \frac{\sqrt{2}}{\pi}, \tag{8}$$

$$e_d|_{\max} = \frac{4}{\pi}, \tag{9}$$

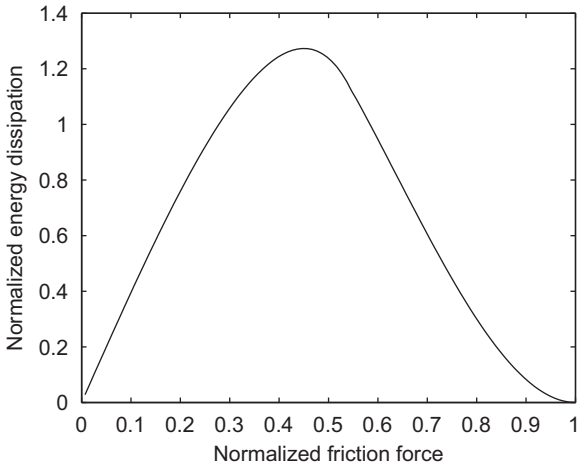

Fig. 2. Normalized energy dissipation vs. normalized friction force.

where e_d is the normalized energy dissipation defined as

$$e_d = \frac{m\omega_0^2 E_d}{F_0^2}. \tag{10}$$

These equations imply that the optimum friction force is independent of the mass and the excitation frequency and only depends on the amplitude of the excitation, which is a well-known fact [4,6,23]. The corresponding maximum normalized energy dissipation is then fixed and independent of the mass and excitation frequency and amplitude. Furthermore, comparing Eqs. (6) and (8) reveals that the maximum energy dissipation occurs in the continuous sliding region ($f_r|_{\max} < f_r|_{\text{threshold}}$). These conclusions hold also for the SDOF system in Fig. 1(a) when $\omega_n/\omega_0 < 1$ and $\xi_n < 0.5$, and the curve of energy dissipation vs. friction force is qualitatively similar to the result shown in Fig. 2.

In the following section the influence of the friction model on the form of the curve in Fig. 2 and on the optimum values given by Eqs. (6) and (8) will be analyzed.

3. Numerical analysis of a periodically forced system with friction

3.1. Influence of stick phase

The stick phase has been modeled using three different friction laws: viscous damping, arctan function and switch model (see [24]). In all three cases a constant friction force is used in the slip phase and $F_s = F_d$. The corresponding equations are:

Viscous damping:

$$f_r = \begin{cases} F_d \operatorname{sgn}(v), & |v| > \eta, \\ \dfrac{F_d}{\eta} v, & |v| \le \eta. \end{cases} \tag{11}$$

Arctan function:

$$F_r = F_d \frac{2}{\pi} \arctan(\varepsilon v). \tag{12}$$

Switch model:

$$F_r = \begin{cases} F_d \operatorname{sgn}(v), & |v| > \eta, \\ \min\{|F_{\text{ex}}|, F_d\} \operatorname{sgn}(F_{\text{ex}}) + \alpha v, & |v| \le \eta. \end{cases} \tag{13}$$

The zero velocity interval η is normally chosen such that $1 \gg \eta > \text{Tol}$, where Tol is the tolerance of the integration method. The parameter ε in the arctan function is the steepness parameter and $\alpha > 0$ is a factor introduced to avoid numerical instabilities in the Switch model [24]. The differential equation that describes the nonlinear non-autonomous system in Fig. 1 is

$$\dot{\mathbf{x}}(t) = \mathbf{A}(t)\mathbf{x}(t) + \mathbf{b}(t) \quad \text{with } \mathbf{x}(t)^{\mathrm{T}} = [x_1(t)\ \dot{x}_1(t)], \tag{14}$$

$$\text{stick phase}: \mathbf{A} = \begin{bmatrix} 0 & 1 \\ 0 & 0 \end{bmatrix}, \quad \mathbf{b} = \begin{bmatrix} 0 \\ \ddot{x}_0(t) \end{bmatrix},$$

$$\text{slip phase}: \mathbf{A} = \begin{bmatrix} 0 & 1 \\ 0 & 0 \end{bmatrix}, \quad \mathbf{b} = \begin{bmatrix} 0 \\ \pm \dfrac{F_r}{m} \end{bmatrix}.$$

The stable periodic solutions of Eq. (14) have been found using a single-point shooting method. Once the periodic solution is known, the energy dissipated per cycle has been determined using Eq. (7).

The switch model with $\eta = 0.001\,\text{m/s}$ and $\alpha = 10\,\text{N s/m}$ gives a result which is almost identical to the analytical solution and the energy dissipated per cycle as a function of the friction force is very much the same as the analytical result shown in Fig. 2. This is the analytical curve plotted in Fig. 3.

The normalized energy dissipation predicted with viscous damping for the stick phase is shown in Fig. 3(a) for several different values of the parameter η, which is given as a function of a reference velocity, $v_0 = F_0/m\omega_0$ (the velocity amplitude of the mass in the absence of friction). As expected, for $\eta = v_0$ the predicted energy dissipation is very different from the analytical result for Coulomb friction and increases as the friction force increases because the viscous damping coefficient increases as well. But as η decreases the energy dissipation converges to the analytical result and for $\eta = 0.001 v_0$ the two curves are nearly the same.

For the case where the arctan function is used to model the stick phase, similar results are obtained as can be seen in Fig. 3(b). In this case the steepness parameter ε has been varied from 1 to 1000. Again the predicted dissipated energy converges rapidly to the analytical result.

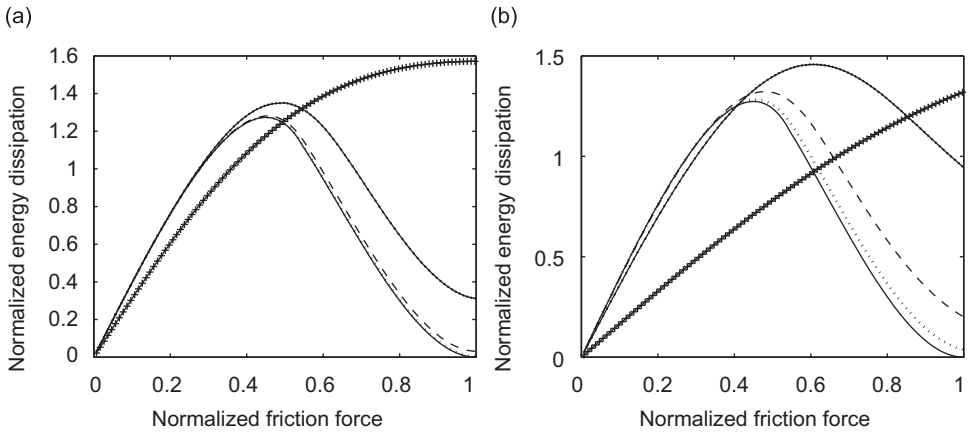

Fig. 3. Normalized energy dissipation vs. normalized friction force. (a) Viscous damping in stick-phase, (b) arctan function in stick-phase. (—) Analytical, (. . .) $\eta/v_0 = 0.001$ resp. $\varepsilon = 1000$, (- - -) $\eta/v_0 = 0.01$ resp. $\varepsilon = 100$, (-.-.-) $\eta/v_0 = 0.1$ resp. $\varepsilon = 10$, (-+-+) $\eta/v_0 = 1$ resp. $\varepsilon = 1$.

It can be concluded that including a small amount of damping in the stick phase has a limited influence on the predicted energy dissipation in the stick–slip region ($f_r \gtrapprox 0.54$) and a negligible influence on the maximum energy dissipation and optimum friction force.

3.2. Influence of slip phase

The slip phase has been modeled as shown below

$$F_r = \begin{cases} g(v)\,\mathrm{sgn}(v), & |v| > \eta, \\ \min\{|F_{ex}|, F_s\}\,\mathrm{sgn}(F_{ex}) + \alpha v, & |v| \le \eta, \end{cases} \tag{15}$$

where $g(v)$ is the Stribeck function. There are different parametrizations of the Stribeck effect as discussed in [24]. In this paper the following expression is chosen:

$$g(v) = F_s[\gamma + (1-\gamma)\mathrm{e}^{-|v/v_s|^{\delta}}], \tag{16}$$

where $v_s > 0$ is called the Stribeck velocity, δ is the shaping parameter of the Stribeck curve and $\gamma = F_d/F_s$ with F_s and F_d the static and dynamic friction force. Other parametrizations have also been considered but are not shown here, since the influence of the parametrization chosen to model the Stribeck effect on the predicted energy dissipation is very small [25].

The parameters δ and v_s determine the decay of the friction force from F_s to F_d. A fixed value of $\delta = 1$ has been chosen and two different values of γ, 0.7 and 0.5, have been considered as was done in [16]. Relationships between energy dissipation and static friction force similar to the one shown in Fig. 2 were derived for $\gamma = 0.7$ and 0.5. Those are the analytical curves shown in Fig. 4. The Stribeck velocity v_s has been varied between 1 and 0.001 m/s, $v_s = 0.001$ m/s gives a very steep decay of the friction force and $v_s = 1$ m/s gives a very slow decay.

The results of the simulations with $v_s = 0.001, 0.01, 0.1, 1$ m/s are shown in Fig. 4(a) for $\gamma = 0.7$ and Fig. 4(b) for $\gamma = 0.5$ and compared to the analytical results from [16]. It should be noted that both plots show the normalized energy dissipation as a function of the normalized *static* friction force. Therefore all curves shift to the right with respect to the curve in Fig. 2 since $F_s > F_d$.

In both cases the dissipated energy curve for $v_s = 0.001$ m/s is very similar to the analytical prediction. This result validates the analytical derivations presented in [16], since it is clear that the numerical prediction converges to the analytical result for very small values of v_s.

For the two values of γ considered, the maximum energy dissipation goes through a minimum, this effect being clearly more pronounced for $\gamma = 0.5$. As v_s increases the optimum friction force decreases by a similar amount for both values of γ. As one would expect, for very large values of v_s the energy dissipation curve tends to the analytical result for $F_s = F_d$. In the parameter range considered, the optimum friction force is more sensitive to variations of v_s than the maximum energy dissipation. In order to evaluate these results knowledge of the parameter values that can be expected in practice is needed.

The friction characteristics of teflon bearings for building isolation are experimentally determined in [18] and values of $v_s = 0.016-0.06$ m/s and $\gamma = 0.74-0.76$ are found. In [19] the parameters of a friction contact between a teflon block and a metal disk are identified to be $\gamma = 0.71$ and $v_s = 0.3$ m/s. In [20] the friction in the joint of a robot arm is identified leading to $v_s = 0.001$ m/s and $\gamma = 0.7$, whereas in [21] $\gamma = 0.68-0.75$ and $v_s = 0.07-0.08$ m/s are reported for a similar system. Finally, $\gamma = 0.8$ and $v_s = 0.02$ m/s are applied in [26] to model a motor-driven inertia subjected to friction and $\gamma = 0.7$ and $v_s = 0.1$ m/s are used in [22] for the design of a nonlinear observer. From the above it can be concluded that values of γ between 0.8 and 0.7 and v_s between 0.01 and 0.1 m/s can be expected in practice. For these values of γ and v_s both the

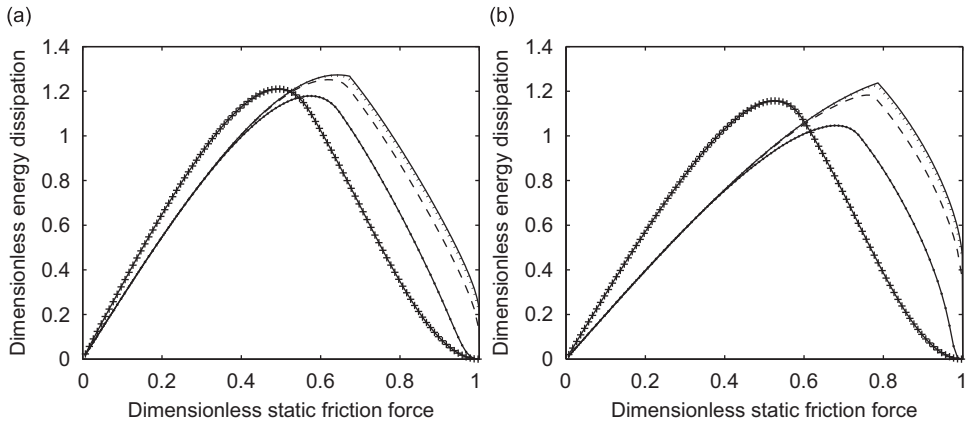

Fig. 4. Normalized energy dissipation vs. normalized friction force. Stribeck1 with $\delta = 1$ and (a) $\gamma = 0.7$, (b) $\gamma = 0.5$. (—) Analytical, (. . .) $v_s = 0.001$, (- - -) $v_s = 0.01$, (-.-.) $v_s = 0.1$, (-+-+) $v_s = 1$.

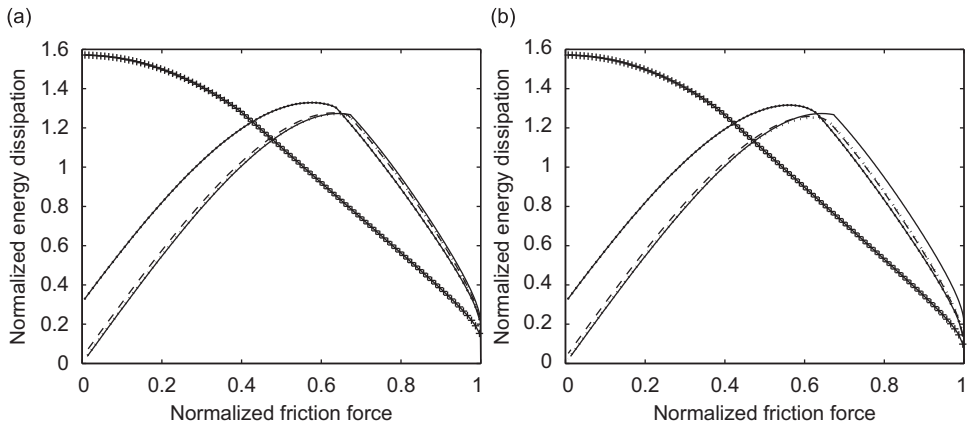

Fig. 5. Normalized energy dissipation vs. normalized friction force. Stribeck1 and viscous damping for $v \neq 0$ with $\gamma = 0.7$, $\delta = 1$ and (a) $v_s = 0.001\,\mathrm{m/s}$, (b) $v_s = 0.01\,\mathrm{m/s}$. (—) Analytical, (. . .) $d = 0.001\,\mathrm{N\,s/m}$, (- - -) $d = 0.01\,\mathrm{N\,s/m}$, (-.-.) $d = 0.1\,\mathrm{N\,s/m}$, (-+-+) $d = 1\,\mathrm{N\,s/m}$.

optimum friction force and the maximum energy dissipation take values within 10 percent of the analytical prediction with Coulomb friction.

In practice, viscous effects are also observed as the relative velocity increases. In order to model these effects a viscous damping term has been added to the Stribeck curve as shown below:

$$F_r = \begin{cases} g(v)\,\mathrm{sgn}(v) + \mathrm{d}v, & |v| > \eta, \\ \min\{|F_{\mathrm{ex}}|, F_s\}\,\mathrm{sgn}(F_{\mathrm{ex}}) + \alpha v, & |v| \leq \eta, \end{cases} \tag{17}$$

where d is the damping coefficient.

The corresponding curves of energy dissipation vs. static friction force can be seen in Figs. 5 and 6 for $\gamma = 0.7, 0.5$ respectively. Results for two values of the Stribeck velocity $v_s = 0.001, 0.01$ are shown with $\delta = 1$. The damping coefficient d has been varied between 0.001 and 1 N s/m.

The main effect of including viscous damping is that the energy dissipated in the continuous sliding region (low static friction force) increases and decreases in the stick–slip region (high static friction force) as the viscous damping coefficient increases. For low values of the static friction force and large values of the viscous damping coefficient ($d = 1\,\mathrm{N\,s/m}$) the viscous term is dominant, which explains why the dissipated energy increases as the static friction force decreases.

The values of the damping coefficient d found in practice [18,21,26–28] are often below 0.1 N s/m. No viscous effects can be seen in the experimental results with teflon bearings for buildings [18,27], $d = 0\,\mathrm{m/s}$. In [21] a viscous damping coefficient d between 0.079 and 0.082 N s/m is found for a rotating arm, while in [26] $d = 0.1\,\mathrm{N\,s/m}$ is applied to the motor-driven inertia with friction. Finally, in [28] a laboratory scale set-up for a drilling system is experimentally studied and a value of $d = 0.01\,\mathrm{N\,s/m}$ is found. For this range of values of d the maximum energy dissipation increases and the optimum

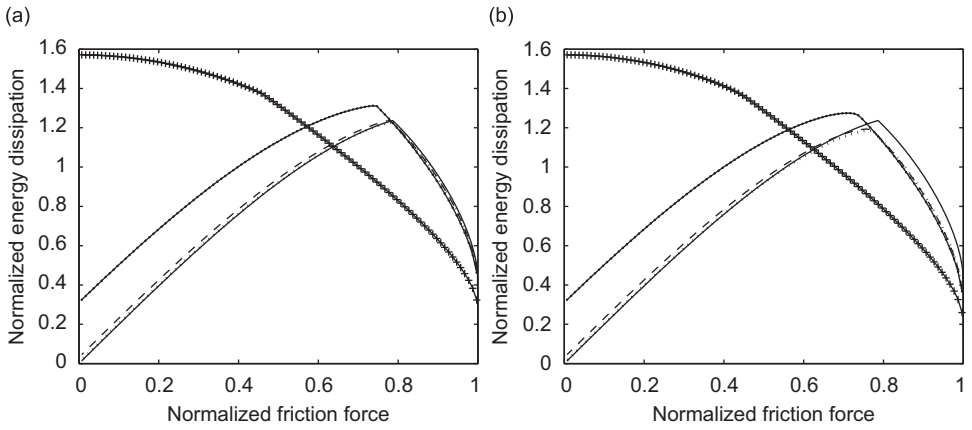

Fig. 6. Normalized energy dissipation vs. normalized friction force. Stribeck1 and viscous damping for $v \neq 0$ with $\gamma = 0.5$, $\delta = 1$ and (a) $v_s = 0.001$ m/s, (b) $v_s = 0.01$ m/s. (—) Analytical, (. ..) $d = 0.001$ N s/m, (- - -) $d = 0.01$ N s/m, (-.-.) $d = 0.1$ N s/m, (-+-+) $d = 1$ N s/m.

friction force decreases as d increases, although these effects are less pronounced than when the Stribeck velocity v_s is varied.

Summarizing, the choice of friction model for the slip phase can have a significant influence on the predicted curve of dissipated energy vs. friction force depending on the parameter values considered in the model. When realistic parameter values for (dry) friction are used, the influence of the friction model is relatively small, being both the predicted maximum energy dissipation and optimum friction force within 10 percent of the analytical values for Coulomb friction.

3.3. Discussion

The results presented in this section show that using of continuous approximations to model the stick phase (viscous damping, arctan function) has little influence on the predicted energy dissipation when values of the parameters representative for dry friction are chosen. It does not seem interesting to use these approximations since the switch model is computationally cheaper and a more realistic model of the stick phase.

The friction model chosen to model the sliding region (Stribeck effect, viscous damping) can have a significant influence on the predicted energy dissipation. The predicted maximum energy dissipation and optimum friction force depend both on the Stribeck velocity v_s and on the viscous damping coefficient d. The optimum friction force is more sensitive to variations of v_s or d than the maximum energy dissipation. However, as discussed in the previous section, in practice one is likely to find values of $\gamma \simeq 0.7$, $0.01 < v_s < 0.1$ m/s and $d < 0.1$ m/s. For these values of the model parameters both the maximum energy dissipation and optimum friction force are within 10 percent of the analytical prediction obtained with the Coulomb model. This leads to the conclusion that the Coulomb friction model might be sufficiently accurate when the goal is to optimize the design parameters of friction dampers with stiff localized contacts and large relative displacements within the contact.

Furthermore, for the abovementioned parameter values the optimum stays in the continuous sliding region. This fact together with the conclusions from the analysis of the stick phase indicates that the exact behavior during the stick-phase will not significantly influence the prediction of the maximum energy dissipation and the optimal friction force. These can be an indication that modeling the pre-sliding behavior with a LuGre type model, for example, might not be necessary for this type of systems. However, the Coulomb model is not suitable for applications where an accurate estimation of the energy dissipation in pre-sliding (stick) phase is required, since it underestimates the energy dissipation in this region.

4. Description of the experiments

4.1. Description of the experimental set-up and measurement procedure

The experimental investigation of energy dissipation of dry friction has been done at a set-up where a shaker forces a sledge back and forth. In Fig. 7 a top-view sketch of the set-up is depicted. As friction lip a steel part is used which is stiff in the translating direction and elastic in the direction perpendicular to the translation. A bearing ball is attached to the part and used as friction tip. The bearing balls slide along a polished silicium–carbonate plate which is fixed to the underground. The normal force between the bearing ball and the plate is adjustable by turning the bolt which pushes a spring. In this set-up the sledge behaves as a free mass in a frequency range from approximately 10–120 Hz.

The data-acquisition and the control of the excitation force is done with a Siglab interface. To excite the sledge periodically by the shaker, a sinusoidal voltage signal is sent from the Siglab interface to a current amplifier. The current

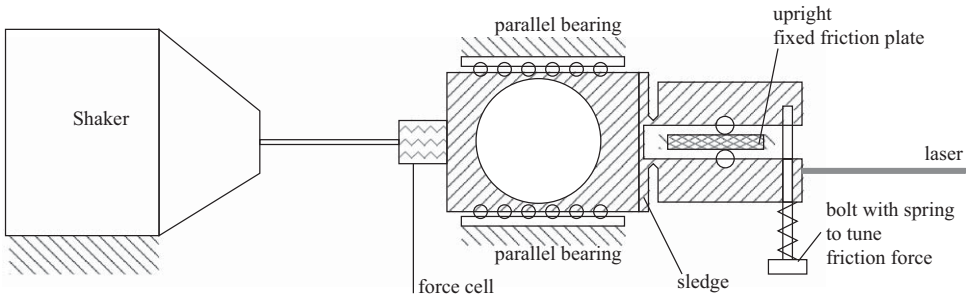

Fig. 7. Top-view of the experimental set-up with the new friction addition.

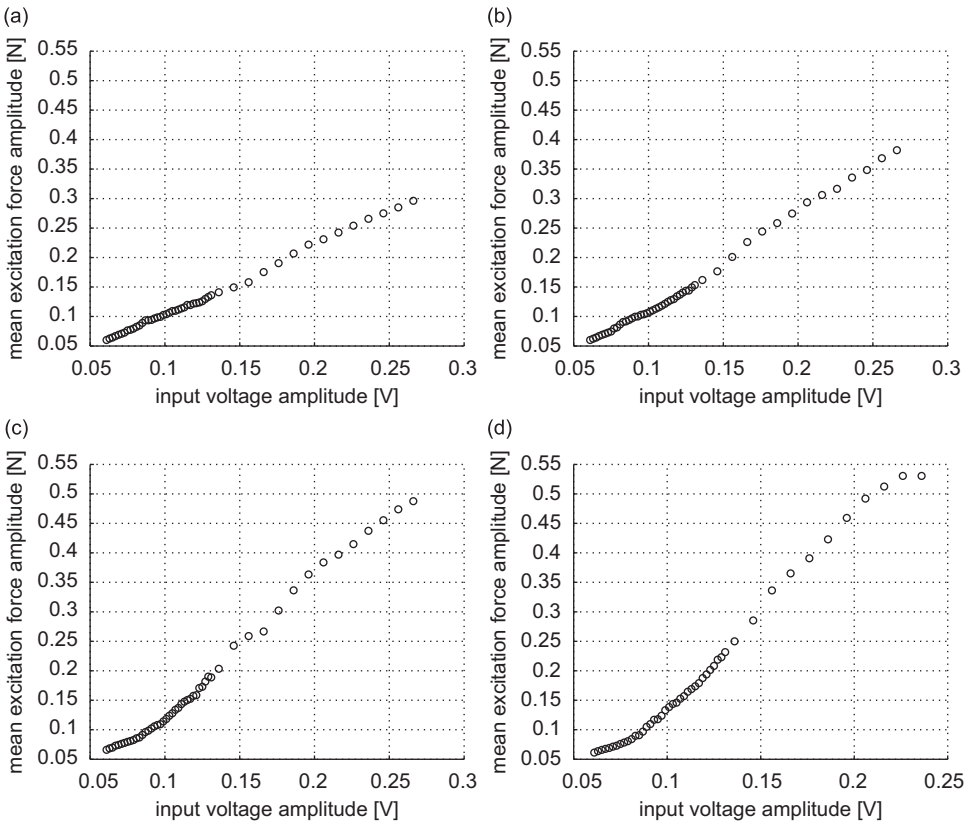

Fig. 8. Force amplitude against input voltage amplitude, (a) 13 Hz, (b) 14 Hz, (c) 15 Hz and (d) 16 Hz.

amplifier transforms the voltage signal to a current signal that is input to the electromechanical shaker. The force cell measures the excitation force acting on the sledge and an acceleration sensor is attached to the sledge. A laser-doppler velocimeter is used to acquire the velocity and the displacement.

The normal force is kept constant during a measurement series but the friction characteristics of the set-up are completely unknown. During an experiment a sinusoidal input signal is used to let the shaker excite the sledge with a periodic force. This force is not sinusoidal, since the force provided by the shaker depends on the impedance of the system (sledge-bearings-friction head) attached to it. At a defined excitation frequency ω_0, the voltage amplitude, V_0, of the sinusoid is increased or decreased in small steps. The variation of normalized friction force ($f_r = F_r/F_0$) is therefore achieved by varying the excitation force F_0 of the shaker on the sledge. The range of the excitation amplitude levels used in the experiments is sufficiently large to ensure that the transition from stick–slip to continuous sliding and the maximum normalized energy dissipation can be observed.

Low excitation frequencies are preferred, because at low excitation frequencies the excitation force amplitude is less sensitive to changes in the input voltage amplitude level. This is shown in Fig. 8, where the mean excitation force amplitude

over 25 cycles is plotted as a function of the input voltage amplitude for four different excitation frequencies. It is clear that the slope of the lines increases as the excitation frequency increases. This is caused by the dynamic behavior of the electromagnetic shaker [29]. As a consequence of this effect, small input voltage variations lead to large excitation force variations at higher frequencies and the stick–slip phase cannot be measured, since the resolution of the measurement system is too coarse to allow for small enough input voltage variations. Therefore the excitation frequency is kept low in order to be able to identify the stick–slip phase and the transition from stick–slip to continuous sliding. The lower limit of the excitation frequency is determined by the fact that below approximately 13 Hz the sledge cannot be modeled as a free-mass anymore.

Measurements are performed at excitation frequencies of 13, 14, 15, 16 and in one measurement series also at 17 and 18 Hz. A series always starts at 13 Hz and the frequency is increased up to the highest frequency. At each excitation frequency the excitation amplitude is first increased and then decreased with small steps. At each excitation voltage amplitude level the actual excitation force on the sledge and the acceleration, velocity and displacement of the sledge are measured for 25 excitation periods. This together is called a measurement series. After one series wear has affected the plate and bearing balls too much to be used again and plate and bearing balls are changed for a new series of measurements. In total four measurement series have been completed to check the repeatability and robustness of the results.

An impression of the measured signals is given in Fig. 9, where the measured force, acceleration, velocity and displacement are plotted for an excitation frequency of 13 Hz and four different input voltage amplitudes. A similar behavior is observed at other excitation frequencies.

In Fig. 9(a) the system is clearly in stick–slip phase. At a higher excitation force, the system passes from stick–slip phase into continuous sliding for an input voltage between 0.109 and 0.115 V. At an input voltage of 0.109 V stick–slip is seen in Fig. 9(b) where the velocity signal is sticking at zero and at the same time the acceleration is zero as well, while at an input voltage of 0.115 V, depicted in Fig. 9(c), a non-zero acceleration signal is measured at the time instant where the velocity is zero which indicates that the system is in continuous sliding. It can also be seen that higher input voltage amplitudes result in a larger phase shift between force and velocity. It is due to this phase-shift that frictional energy dissipation occurs. The

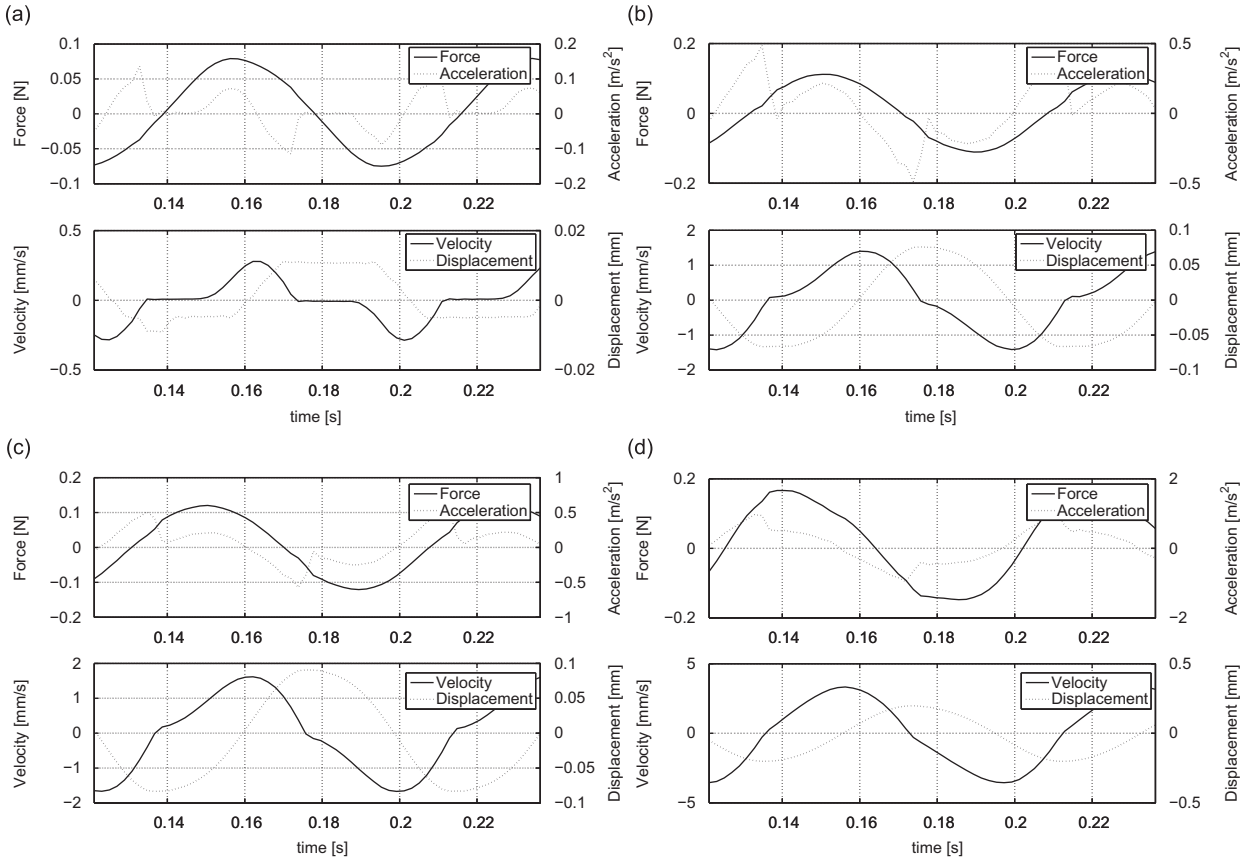

Fig. 9. Time plots of force and acceleration, velocity and displacement for different input amplitude voltage level at a frequency of 13 Hz. (a) 0.077 V, (b) 0.109 V, (c) 0.115 V, (d) 0.156 V.

phase-shift between velocity and force at maximum energy dissipation, in Fig. 9(d), is about 0.01 s which is about one-eight of the period. This value is in good agreement with the theoretical value for the free mass model given in [16], where an optimum phase-shift of $\pi/4$ is found.

The force of the shaker to the sledge is not a perfect sine wave. This is due to the fact that the exerted force is altered by the velocity and friction forces on the sledge. This deviation from the sine wave is not problematic for the current study as long as the force is periodic. Moreover, the amplitude of the force is nonlinear with the amplitude of the input voltage control signal. This is not considered a problem since the actual excitation force is measured.

4.2. Calculation of normalized energy dissipation and the normalized friction force

In the measured frequency range the experimental set-up can be modeled as a free mass excited by a periodic force as in Fig. 1. The friction force can be calculated from

$$F_r(t) = F_0(t) - ma(t), \tag{18}$$

where $F_0(t)$ is the measured force on the sledge, m is the mass and $a(t)$ the measured acceleration of the sledge. The dissipated energy is calculated with the following expression:

$$E_d = \frac{\Delta t}{n} \sum_{k=1}^{n \cdot P} F_r(t_k) v(t_k), \tag{19}$$

where P is the number of time samples in one period, n is the number of periods measured, $v(t)$ the velocity of the sledge and Δt is the sampling time. This energy dissipation can be normalized by applying (10), where the amplitude of the excitation force is calculated as follows:

$$F_0 = \frac{1}{2n} \sum_{i=1}^{n} \max(F_0(t_k)) - \min(F_0(t_k)) \quad \text{with } k = (i-1)P + 1, \ldots, iP. \tag{20}$$

To obtain the normalized friction force, $f_r = F_r/F_0$, the expression for the normalized friction force at the threshold of stick–slip to continuous sliding given in (6) has been applied. The normalized friction force has been determined based on the excitation force at the threshold of stick–slip to continuous sliding $F_0|_{\text{threshold}}$. The threshold is determined by comparing the acceleration and velocity signals. Stick is observed if the acceleration signal crosses zero when the velocity is zero. The accuracy of the estimated friction force is limited by the increments used for the excitation amplitudes and the sample frequency. The transition from stick–slip to continuous sliding occurs often at the same excitation force for all periods. The friction force can then be estimated from $f_r|_{\text{threshold}} \times F_0|_{\text{threshold}}$ and the normalized friction force becomes

$$f_r = \frac{f_r|_{\text{threshold}} \times F_0|_{\text{threshold}}}{F_0}. \tag{21}$$

In the next section the experimentally determined normalized energy dissipation from Eqs. (10) and (19) is plotted as a function of the normalized friction force obtained from (21) and compared to the analytical result from [16] (see Fig. 2).

5. Comparison of calculated and measured energy dissipation

It has already been mentioned that four measurement series have been completed and that, for each measurement series different excitation frequencies have been measured. The experimentally determined energy dissipation for the excitation frequencies of 13 and 16 Hz is compared to the analytical curve in Figs. 10 and 11, respectively. The results for the four measurement series are shown. In every plot a distinction is made between decreasing and increasing normalized friction force and between the stick–slip and continuous sliding regions. Note that a decreasing normalized friction force corresponds to an increasing excitation force and vice versa. The continuous solid line corresponds to the theoretically determined normalized energy dissipation from [16].

In general a very good agreement is found between the experimentally determined friction force and the theoretical results. The experimental results follow the theoretical curve nicely in most cases and the results are repeatable. Deviations are seen mostly in the stick–slip region (higher values of f_r), where the experimentally determined normalized energy dissipation is often higher than the predicted value. This can be explained by the difficulty to perform accurate measurements in this region and possibly by viscous effects as has been shown in Section 3.1. An exception to this behavior is found in Fig. 11(a), where the experimentally determined energy dissipation suddenly drops to values below the theoretical curve in the stick–slip region. This might be due to a difference between the static and dynamic friction force in the set-up, as shown in [16].

In the continuous sliding region (lower values of f_r) the experimentally determined values show a good agreement with the theory except for the result in Fig. 10(d) with increasing excitation force. In this case, the measured values are well below the predicted normalized energy dissipation. A close look reveals that the optimum normalized friction force is also higher than the theoretical value. This together with the fact that it was not possible to measure the stick–slip region in this

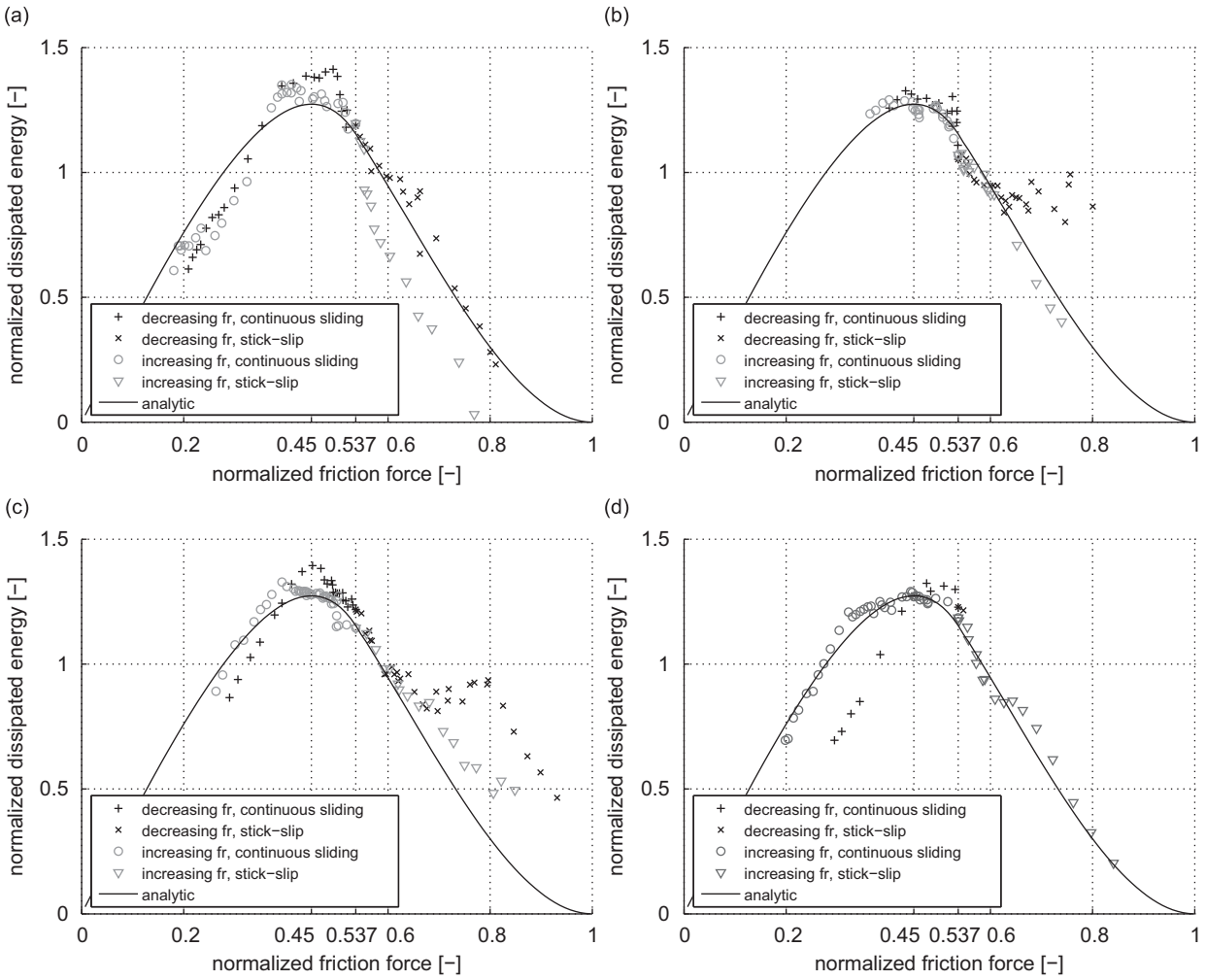

Fig. 10. Normalized energy dissipation against normalized friction force at 13 Hz for four different measurement series, (a) A, (b) B, (c) C, (d) D.

case lead to the conclusion that the discrepancies might be due to an error in determining $F_0|_{\text{threshold}}$ in (21) and, therefore, to an error in the scaling of the normalized friction force.

When looking at the results in Figs. 10 and 11 one should bear in mind that before each measurement series the friction plate and bearings are replaced and that the normal force is manually adjusted by fastening the bolt shown in Fig. 7. No care has been taken to achieve a given normal force, which means that the actual friction force can vary from one measurement series to the next and this is probably the case. Therefore, the fact that the measured maximum energy dissipation does not significantly change for the different measurement series leads to the conclusion that the maximum normalized energy dissipation does not depend on the actual value of the friction force, as predicted in Eq. (9).

Comparing Figs. 10 and 11 leads to the conclusion that the excitation frequency has no influence on the normalized energy dissipation, as was expected from theory. This can be more clearly seen in Fig. 12 where the experimentally determined normalized energy dissipation is plotted for six different excitation frequencies within one measurement series. Again a distinction is made between decreasing and increasing friction force and the stick–slip and continuous sliding regions. The theoretical normalized energy dissipation is given by the solid line as before. It can be concluded that the normalized energy dissipation as a function of the normalized friction force is roughly independent of the excitation frequency. Furthermore, the difference between the experimentally determined maximum normalized energy dissipation and the value predicted from (9) is less than 10 percent in all cases and the corresponding optimum normalized friction force is approximately equal to the predicted value.

Finally, the results in Fig. 12 show that the experimentally determined normalized energy dissipation in the stick–slip region is significantly larger than the theoretical curve for most excitation frequencies. The possible reasons for this discrepancy will be discussed in the next section.

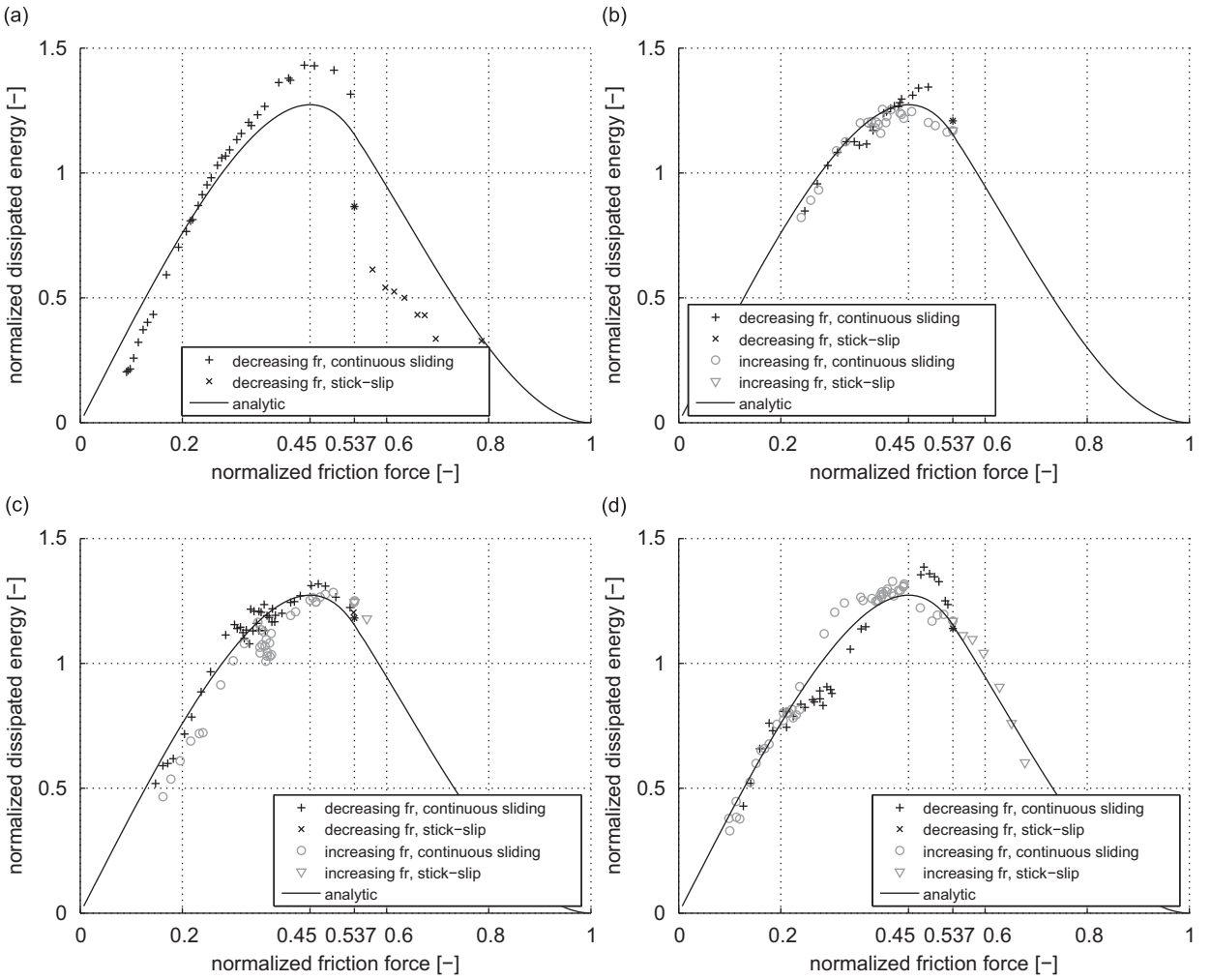

Fig. 11. Normalized energy dissipation against normalized friction force at 16 Hz for four different measurement series, (a) A, (b) B, (c) C, (d) D.

6. Discussion

The experimental results of the previous section show a very good agreement with the results from the analytical model presented in [16]. This is a remarkable result, since the theoretical results have been obtained for the most simple form of friction model, namely Coulomb friction, and the friction model that best describes the set-up is not known. This result validates the conclusions derived in Section 3, where numerical experiments for different friction models are reported and it is shown that the normalized energy dissipation vs. normalized friction force is relatively insensitive to the choice of friction model. In particular, the optimum value of the friction force and the maximum normalized energy dissipation seem to be rather robust, since approximately the same maximum energy dissipation and optimum friction force is found in all experiments (four measurement series, six different excitation frequencies). It should be noted that the friction plate and the bearing balls are replaced after each measurement series, which means that variations in the friction force can be expected.

The main discrepancies between experiments and theory are found in the stick–slip region (higher values of f_r). This could be due to the difficulties to perform accurate and repeatable measurements in this region, but it is more likely that the larger energy dissipation measured is due to the presence of viscous damping in the system. Possibly the lubrication oil in the linear bearings introduces a small amount of viscous damping and this leads to an increase of energy dissipation in the stick phase (see Fig. 3(a)).

It is clear that the effect of viscous damping is to increase the energy dissipation in the stick–slip region. Therefore the higher normalized energy dissipation values found in the experiments can partly be explained by viscous damping. However, viscous damping does not explain the fact the normalized energy dissipation seems to stay at a constant value in

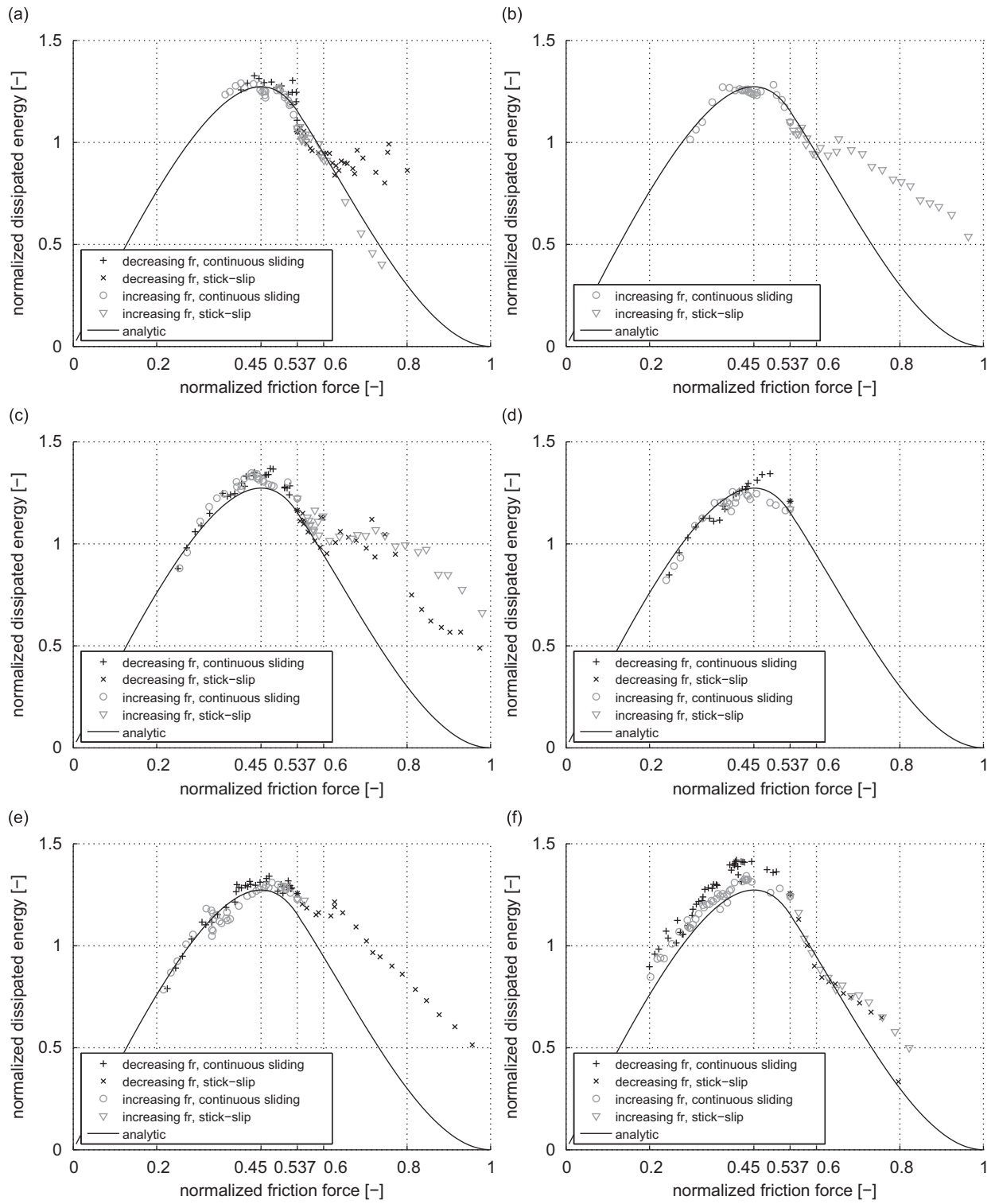

Fig. 12. Normalized energy dissipation against normalized friction force for measurement series B, (a) 13 Hz, (b) 14 Hz, (c) 15 Hz, (d) 16 Hz, (e) 17 Hz and (f) 18 Hz.

the region $0.6<f_r<0.8$. Applying a LuGre type model to model the stick phase would probably lead to a better correlation between theory and experiments in this region. However, this type of models have not been investigated since this paper focuses on the optimum friction force and maximum energy dissipation, which for the SDOF system studied are correctly predicted by the Coulomb friction model.

7. Conclusions

In the present paper the influence of the friction model on the predicted energy dissipation has been investigated by means of numerical models and experiments on a free mass with friction. The free mass system with friction is chosen for its simplicity and ease of implementation, but it can be shown that for a wide range of parameter values the qualitative behavior of the free mass regarding the energy dissipated as a function of the friction force is similar to that of the mass–spring–damper systems often used to model friction dampers.

The numerical simulations indicate that the curve of energy dissipation vs. friction force depends on the friction model chosen. However, for the parameter values found in practice the optimum friction force and maximum energy dissipation stay within 10 percent of the predicted values from the analytical model with Coulomb friction. These results lead to the conclusion that the Coulomb friction model might be sufficient when the goal is to optimize the friction force and maximize the energy dissipated in friction dampers with stiff localized contacts and large relative displacements within the contact.

In order to test the above conclusion the energy dissipation through friction for a free mass excited by a periodic force has been experimentally determined and compared to theoretical results from a model with Coulomb friction. The measured energy dissipation is in excellent agreement with the energy dissipation predicted by the model. This is a remarkable result, since the theoretical results have been obtained for the most simple form of friction model, namely Coulomb friction, and the friction model that best describes the set-up is not known. Furthermore, the measured maximum energy dissipation and the corresponding optimum friction force agree within 10 percent with the theoretical prediction. This result is particularly interesting because no care has been taken to ensure predetermined friction characteristics and variations in friction force between each measurement series are very likely. Therefore the maximum energy dissipation and optimum friction force are relatively robust properties of the system, as expected from the theoretical analysis.

It can be concluded that for the SDOF system studied Coulomb friction gives a good estimation of the maximum energy dissipation and optimal friction force. Based on these results the Coulomb friction model can be expected to give realistic predictions of the performance of friction dampers with stiff localized contacts and large relative displacements within the contact.

Acknowledgments

The authors would like to thank Dr. Pieter Nuij for his advice and assistance in setting up the experiments and Coen Blok for carrying them out.

References

[1] J.G.C.H. Menq, J. Bielak, The influence of microslip on vibratory response, part i: a new microslip model, *Journal of Sound and Vibration* 107 (2) (1986) 279–293.
[2] J. Miller, D. Quinn, A two-sided interface model for dissipation in structural systems with frictional joints, *Journal of Sound and Vibration* 321 (1) (2009) 201–219.
[3] T. Cameron, J. Griffin, R. Kielb, T. Hoosac, Integrated approach for friction damper design, *ASME Journal of Vibration, Acoustics, Stress, and Reliability in Design* 112 (2) (1990) 175–182.
[4] A. Ferri, Friction damping and isolation systems, *ASME Journal of Mechanical Design* 117 (1995) 196–206.
[5] R. Jangid, Optimum frictional elements in sliding isolation systems, *Computers and Structures* 76 (5) (2000) 651–661.
[6] K. Popp, L. Panning, W. Sextro, Vibration damping by friction forces: theory and applications, *Journal of Vibration and Control* 9 (3–4) (2003) 419–448.
[7] A. Bhaskararao, R. Jangid, Harmonic response of adjacent structures connected with a friction damper, *Journal of Sound and Vibration* 292 (4) (2006) 710–725.
[8] T.S.R.K.J. Szwedowicz, C. Gibert, Numerical and experimental damping assessment of a thin-walled friction damper in the rotating setup with high pressure turbine blades, *ASME Journal of Engineering for Gas Turbines and Power* 130 (1) (2008) 012502-1, 012502-10.
[9] F. Sorge, Damping of rotor conical whirl by asymmetric dry friction suspension, *Journal of Sound and Vibration* 321 (1) (2009) 79–103.
[10] T.S.C.W. Stammers, Vibration control of machines by use of semi-active dry friction damping, *Journal of Sound and Vibration* 209 (4) (1998) 671–684.
[11] E. Guglielmino, K. Edge, A controlled friction damper for vehicle applications, *Control Engineering Practice* 12 (2004) 431–443.
[12] I. Lopez, Theoretical and Experimental Analysis of Ring-damped Railway Wheels, Ph.D. Thesis, Universidad de Navarra, Spain, November 1998.
[13] J. Brunel, P. Dufrenoy, F. Demilly, Modelling of squeal noise attenuation of ring damped wheels, *Applied Acoustics* 65 (2004) 457–471.
[14] R. Ibrahim, Recent advances in nonlinear passive vibration isolators, *Journal of Sound and Vibration* 314 (3) (2008) 371–452.
[15] A.R.M.C. Constantinou, A. Mokha, Teflon bearings in base isolation. ii. Modeling, *Journal of Structural Engineering* 116 (2) (1990) 455–474.
[16] I. Lopez, J.M. Busturia, H. Nijmeijer, Energy dissipation of a friction damper, *Journal of Sound and Vibration* 278 (3) (2004) 539–561.
[17] N. Do, A. Ferri, Energy transfer and dissipation in a three-degree-of-freedom system with Stribeck friction, in: *ASME 2005 International Mechanical Engineering Congress and Exposition*, Orlando, Florida, 2005, pp. 195–204.
[18] A.R.A. Mokha, M.C. Constantinou, Further results on frictional properties of teflon bearings, *Journal of Structural Engineering* 117 (2) (1991) 622–626.
[19] D.D.D.H.M. Feemster, P. Vedagarbha, Adaptive control techniques for friction compensation, *Mechatronics* 9 (1999) 125–145.
[20] R. Hensen, M. van de Molengraft, M. Steinbuch, Frequency domain identification of dynamic friction model parameters, *IEEE Transactions on Control Systems Technology* 10 (2) (2002) 191–196.

[21] D. Putra, Control of Limit Cycling in Frictional Mechanical Systems, Ph.D. Thesis, Eindhoven University of Technology, Netherlands, 2004.
[22] P. Bigras, Reduced nonlinear observer for bounded estimation of the static friction model with the Stribeck effect, *Systems and Control Letters* 58 (2009) 119–123.
[23] R. Ibrahim, Friction-induced vibration, chatter squeal, and chaos. Part ii: dynamics and modeling, *Applied Mechanics Review: Dynamics and modeling* 47 (7) (1994) 227–253.
[24] R. Leine, H. Nijmeijer, *Dynamics and Bifurcations of Non-Smooth Mechanical Systems*, Springer, Wiley, 2004.
[25] I. Lopez, H. Nijmeijer, How important is the friction model on the modeling of energy dissipation?, *ENOC-2005*, Vol. 6, Eindhoven, Netherlands, 2005, pp. 363–368.
[26] R. Hensen, M. van de Molengraft, M. Steinbuch, Friction induced hunting limit cycles: a comparison between the LuGre and switch friction model, *Automatica* 39 (12) (2003) 2131–2137.
[27] A.R.M.C. Constantinou, A. Mokha, Teflon bearings in base isolation. ii: testing, *Journal of structural engineering* 116 (2) (1990) 438–454.
[28] N. Mihajlović, Torsional and Lateral Vibrations in Flexible Rotor Systems with Friction, Ph.D. Thesis, Eindhoven University of Technology, Netherlands, 2005.
[29] G.F. Lang, Electrodynamic shaker fundamentals, *S.V. Sound and Vibration* 31 (4) (1997) 14–23.